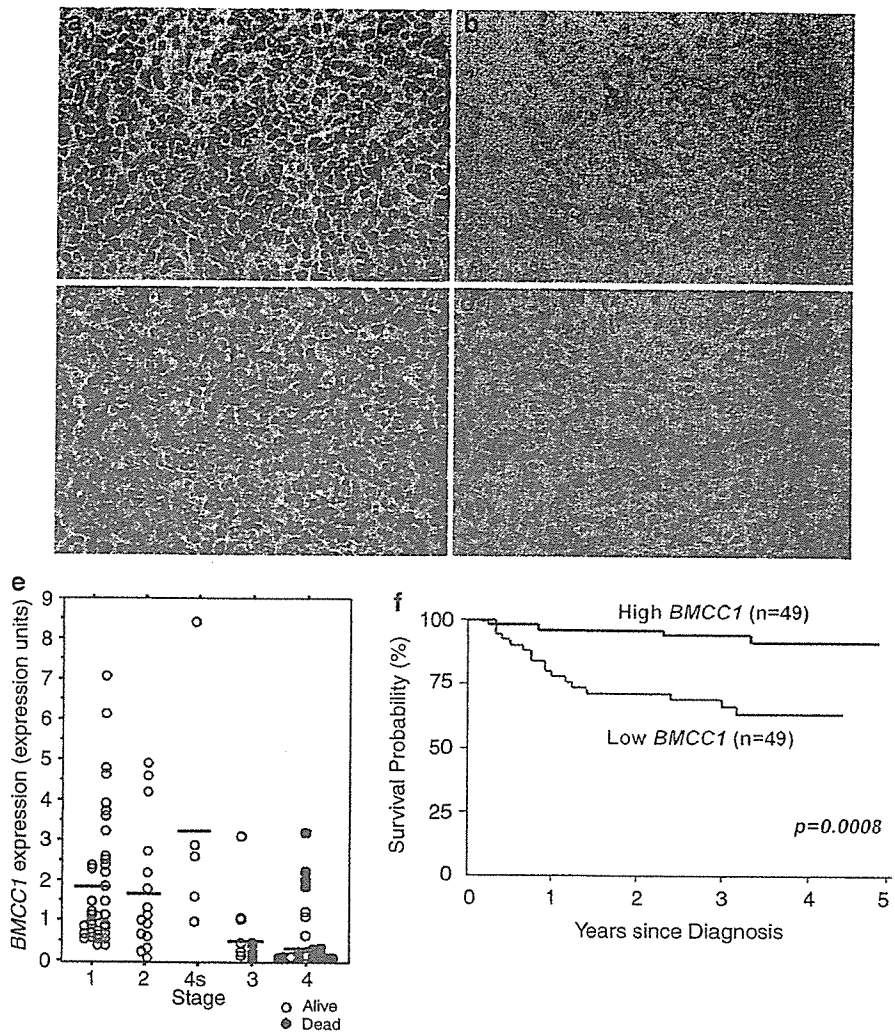

Figure 4 Immunohistochemistry and prognostic significance of BMCC1 expression in primary neuroblastomas. (**a**) and (**b**) In the favorable neuroblastoma without *MYCN* amplification, the tumor cells are occasionally positive for BMCC1 in the cytoplasm. (**c**) and (**d**) The unfavorable neuroblastoma with *MYCN* amplification is negative for BMCC1. (**a**) and (**c**) Hematoxylin–eosin staining. (**b**) and (**d**) BMCC1 immunostaining. (**e**) Low expression of *BMCC1* is associated with poor prognosis of the patients with neuroblastoma. Real-time quantitative RT–PCR analysis of *BMCC1* in 98 tumor samples from patients with neuroblastomas according to tumor stage. The levels of expression of *BMCC1* were normalized to that of *GAPDH*. Horizontal lines; group means, open circles; patients alive, solid circles, patients deceased. (**f**) Cumulative survival curves of patients with neuroblastoma, according to expression of *BMCC1* mRNA. The Kaplan–Meier curves show the probability of survival in terms of the level of expression of *BMCC1*. The survival curves were analysed by the Mantel–Haenszel log-rank test.

RT–PCR (Figure 6a) and Western blot (data not shown). The treatment of the transgenic SCG neurons with NGF in primary culture induced neurite extension similarly to control cells, but induction of apoptosis after depleting NGF was significantly enhanced in the cells overexpressing BMCC1 (Figure 6b–d). This suggested that BMCC1 overexpression may function as proapoptotic in neuronal cells.

Discussion

The presence of the highly conserved BCH domain in BMCC1 suggests its role in the regulation of apoptosis. BNIP2, which shares the BCH domain with BMCC1, has originally been identified as a molecule interacting with the adenovirus E1B 19-kDa protein. The E1B protein protects the cells from apoptosis induced by viral infection or other proapoptotic stimuli (Gooding *et al*., 1991; Hashimoto *et al*., 1991; White *et al*., 1992; Boyd *et al*., 1994). Bcl-2 and its related antiapoptotic proteins can functionally substitute for the E1B 19-kDa protein and bind to BNIP2. Therefore, it has been suggested that BNIP2 is a potential proapoptotic protein (Subramanian *et al*., 1995).

On the other hand, Cdc42 regulates the activation of the c-Jun amino-terminal kinase (JNK) in various cells (Bagrodia *et al*., 1995; Coso *et al*., 1995; Zhang *et al*., 1995). Cdc42 induces an apoptosis mediated by the JNK–MAP kinase cascade in Jurkat T lymphocytes (Chuang *et al*., 1997). The apoptosis is prevented by inhibitors of caspases, suggesting that activation of the

Table 1 Prognostic significance of *BMCC1* expression, age, stage, *TrkA* expression, *MYCN* amplification, mass screening and tumor origin in primary neuroblastomas (log-rank tests)

Variable	*t-tests*			*Log-rank tests*		
	Number of patients	*Mean±s.e.m. (BMCC1 exp.)*	P-*value*	*Number of deaths*	*Number of expected deaths*	P-*value*
BMCC1 expression						0.0008
Low	49			17	9.39	
High	49			4	11.61	
Age (year)						<0.00005
<1	63	1.82±0.23	<0.00005	5	14.55	
⩾1	35	0.64±0.15		16	6.45	
Tumor stage						<0.00005
1, 2, 4s	59	1.97±0.23	<0.00005	0	14.57	
3, 4	39	0.55±0.13		21	6.43	
TrkA *expression*						<0.00005
Low	44	0.91±0.22	<0.00005	21	7.75	
High	54	1.81±0.25		0	13.25	
MYCN *copy number*[a]						<0.00005
Amplified	27	0.30±0.10	<0.00005	18	4.14	
Single	70	1.80±0.20		3	16.86	
Mass screening						<0.00005
Positive	55	1.87±0.22	<0.0025	1	13.32	
Negative	43	0.80±0.22		20	7.68	
Origin						0.061
Adrenal gland	62	1.11±0.20	<0.00005	17	12.82	
Others	36	1.91±0.25		4	8.18	

[a]One patient who had missing *MYCN* information was excluded from analysis.

JNK pathway by Cdc42 is regulated by caspases. The interactive regulation between activation of JNK pathway and that of caspase cascade has also been reported in other biological systems (Cahill *et al*., 1996; Juo *et al*., 1997; Lenczowski *et al*., 1997; Seimiya *et al*., 1997). Cdc42 is also known to function as an initiator of neuronal cell death by activating a c-Jun-regulated transcriptional machinery (Bazenet *et al*., 1998). Cdc42GAP is a Cdc42-activating protein and, like Cdc42, binds to BNIP2 through the BCH domain when it is dephosphorylated at the tyrosine residue. Thus, the proteins with the BCH domain including BMCC1 seem to function in the regulation of apoptosis. The 'EYV' motif in the BCH domain, which is necessary for binding BNIP2 and Cdc42, is also conserved in the same domain of BMCC1. The role of P-loop in the regulation of apoptosis may also be important. Recently, it has been reported that ARTS (apoptosis-related protein in the TGF-β signaling pathway) mediates apoptosis through its P-loop motif. ARTS is a member of the septin family, localizes in cellular mitochondria and plays a role in regulating apoptosis. The P-loop consensus sequence is found in the proapoptotic protein, Apaf-1/CED-4 (Yuan and Horvitz, 1992; Zou *et al*., 1997; Larisch *et al*., 2000). It is interesting that BMCC1 also possesses a P-loop motif, also suggesting its proapoptotic function.

The biological importance of BNIP2 has been reported in the neuronal system. Expression of BNIP2 is developmentally regulated during the maturation of rat brain (Zou *et al*., 1997). The recent reports suggest that expression of *BNIP2* is downregulated by the treatment of NBL cells with estrogen (Garnier *et al*., 1997), and that both estrogen and progesterone promote survival of NBL cells through the BNIP2 function during the apoptosis induced by TNF-α (Vegeto *et al*., 1999). Furthermore, BNIP2 has been identified to be a putative downstream substrate of the FGF receptor tyrosine kinase signaling and possesses GTPase-activating activity to Cdc42. Thus, BNIP2 as well as Cdc42GAP seems to play a role in controlling the intracellular signals of neuronal differentiation and apoptosis.

However, our present results show that, among the molecules with the BCH domain, only *BMCC1*, but not *BNIP2* or *Cdc42GAP*, is differentially expressed among the NBL subsets, significantly at higher levels in favorable tumors than the aggressive ones. This suggests that *BMCC1*, rather than *BNIP2* or *Cdc42GAP*, is functioning *in vivo* in favorable NBLs undergoing neuronal differentiation and/or programmed cell death. The importance of *BMCC1* in NBL cell death has also been demonstrated in the study using neuronal cell lines. The RA-induced apoptosis of CHP134 NBL cells is accompanied with increased expression of *BMCC1*, while induction of differentiation in RTBM1 cells rather decreases its mRNA level. In the former system, the RA-triggered apoptosis induced upregulation of both

Table 2 Cox regression models using *BMCC1* expression and dichotomous factors of age, *MYCN* amplification, mass screening and tumor origin ($n=98$)

Model	*Variable*	P-*value HR (95% CI)*	*Variable*	P-*value HR (95% CI)*	*Variable*	P-*value HR (95% CI)*
A	*BMCC1* exp. (log)	<0.0005 0.53 (0.40, 0.70)				
B	Age (≥1 vs <1 year)	<0.0005 7.5 (2.72, 20.7)				
C	*MYCN* (1 copy vs >1 copy)	<0.0005 0.035 (0.0099, 0.12)				
D	Mass screening (+ vs −)	<0.0005 0.028 (0.0037, 0.21)				
E	Origin (adrenal vs others)	0.072 2.7 (0.91, 8.08)				
F	*BMCC1* exp. (log)	0.007 0.55 (0.47, 0.89)	Age (≥1 vs <1 year)	0.018 3.9 (1.26, 12.0)		
G[a]	*BMCC1* exp. (log)	0.72 1.05 (0.77, 1.47)	*MYCN* (1 copy vs >1 copy)	<0.0005 0.03 (0.0071, 0.13)		
H	*BMCC1* exp. (log)	0.079 0.77 (0.57, 1.03)	Mass screening (+ vs −)	0.003 0.04 (0.0053, 0.34)		
I	*BMCC1* exp. (log)	<0.0005 0.55 (0.41, 0.74)	Origin (adrenal vs others)	0.59 1.38 (0.42, 4.46)		
J	*BMCC1* exp. (log)	0.027 0.59 (0.49, 0.96)	Age (≥1 vs <1 year)	0.014 4.1 (1.33, 12.9)	Origin (adrenal vs others)	0.403 1.5 (0.51, 5.32)

[a]One patient who had missing *MYCN* information excluded from the analysis. All variables were grouped into two categories, except *BMCC1* expression (log). HR, hazard ratio; 95% CI, confidence interval.

p21^{WAF1} and *caspase-3*, and downregulation of survivin. The downregulation and upregulation of *BMCC1* expression was also observed in the newborn mouse SCG cells undergoing NGF-induced differentiation and NGF-depletion-induced apoptosis in primary culture, respectively. Furthermore, in SCG neurons obtained from newborn transgenic mice for *BMCC1*, NGF-depletion-induced apoptosis was significantly enhanced. Thus, these results strongly suggest that *BMCC1* is stimulated or acts as a proapoptotic factor when the neuronal cell death is induced.

BMCC1 mRNA is induced at G1 phase of the cell cycle. The physiological significance of the cell cycle-dependent expression of *BMCC1* is currently unclear. However, activated Cdc42, a BMCC1-related molecule, also induces G1 cell cycle progression in quiescent Swiss 3T3 fibroblasts (Yamamoto *et al*., 1993; Olson *et al*., 1995) and upregulates E2F transcriptional activity in NIH3T3 cells to induce accumulation of cyclin D1 and hyperphosphorylation of RB protein (Gjoerup *et al*., 1998). BMCC1 may also play a role in G1-phase progression of the cell cycle via unknown mechanism.

Our statistical analysis has strongly suggested the importance of *BMCC1* expression in predicting the prognosis of NBLs. The *BMCC1* expression is upregulated in favorable NBLs and downregulated in unfavorable, advanced stages of NBLs. The similar pattern of expression in NBLs has also been reported in *TrkA* (Nakagawara *et al*., 1993, 1994; Nakagawara, 1998, 2001), *c-Ha-Ras* (Tanaka *et al*., 1998), *CD44* (Favrot *et al*., 1993) and *pleiotrophin* (Nakagawara *et al*., 1995). Here, we have added expression of BMCC1, at either mRNA or protein level, as a new prognostic indicator of favorable NBLs. Furthermore, our preliminary result has suggested that activated TrkA physically interacts with BMCC1, which in turn regulates the downstream signaling to control growth, differentiation and survival of neuronal cells (unpublished data). Therefore, BMCC1 could be a key regulator of TrkA-activation-mediated intracellular signaling pathway in favorable NBLs, that is defective in aggressive tumors such as those with *MYCN* amplification. Thus, BMCC1 might be an important molecular tool to develop new therapeutic strategy against aggressive NBLs.

Materials and methods

Patients

We studied tumors from 98 children with NBL which had been diagnosed between 1995 and 1999. In all, 55 patients were

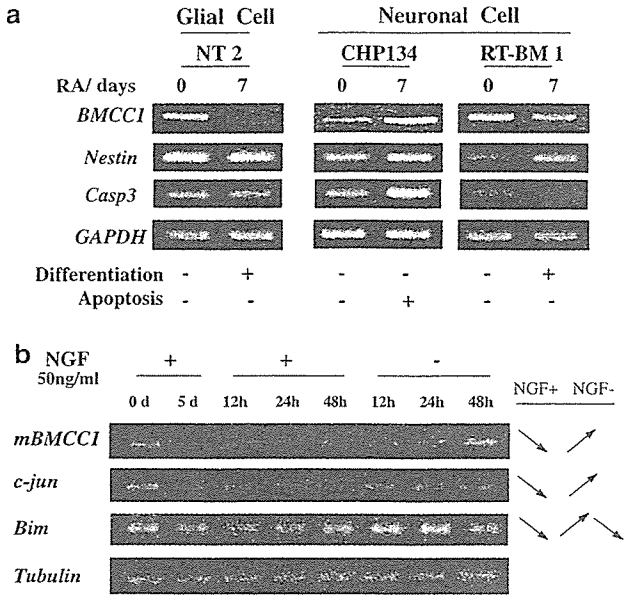

Figure 5 Expression of *BMCC1* during differentiation and apoptosis on neuronal cells. (**a**) The changes in *BMCC1* expression during induction of differentiation and apoptosis in neuronal cell lines. Two neuroblastoma cell lines (CHP134 and RTBM1) and teratocarcinoma cell line NT2 were treated with 5 μM all-*trans* retinoic acid (RA) or were cultured in the serum-free RPMI1640 medium for 7 days. Semiquantitative RT–PCR was performed using *BMCC1* primers and control *GAPDH* primers. (**b**) The changes in mRNA expression of mouse *BMCC1* during NGF-induced differentiation and NGF-depletion-induced apoptosis. Mouse superior cervical ganglion (SCG) cells were cultured with NGF for 5 days and were further cultured with or without NGF for indicated intervals (12, 24 and 48 h) (see Figure 6b, upper panels). *Tubulin* primers were used for standardization of the cDNA concentration for semiquantitative RT–PCR. *c-jun* and *Bim* were also used for positive controls.

identified by a MS program started in 1985. The selection of tumors for this study was solely based on the availability of a sufficient amount of tumor tissue, from which DNA and RNA could be prepared for the analyses described below. The diagnosis of NBL was confirmed by histologic assessment of the tumor specimen obtained at surgery according to the Shimada's classification (Shimada *et al*., 1984). The tumors were staged according to the International NBL Staging System (INSS) (Brodeur *et al*., 1993). In all, 39 tumors were stage 1, 15 stage 2, five stage 4, 10 stage 3 and 29 stage 4. The patients were treated according to the protocols previously described (Kaneko *et al*., 1998).

Tumor samples and cell lines

Fresh, frozen tumorous tissues were sent to the Division of Biochemistry, Chiba Cancer Center Research Institute, from various hospitals in Japan with informed consent from the patients' parents. All samples were obtained by surgery (or biopsy) and stored at −80°C. Studies were approved by the Institutional Review Board of the Chiba Cancer Center. Human cell lines which we used, except for COS-7, HEK 293 and HeLa cells, were cultured in the RPMI1640 medium (Nissui Pharmaceutical Co. Ltd, Tokyo, Japan) with 10% fetal bovine serum (FBS, Invitrogen Corp.) and 50 μg/ml penicillin/streptomycin (Invitrogen Corp.) at humidified 5% CO_2/95% air at 37°C. COS-7, HEK 293, and HeLa cells were grown in Dulbecco's modified Eagle's medium (DMEM) supplemented with 10% (v/v) FBS, 2 mM L-glutamine (Nissui Pharmaceutical Co. Ltd), 50 U/ml penicillin, and 50 μg/ml streptomycin.

Treatment of cell lines with RA

NT2, CHP134 and RTBM1 were seeded at a density of 1×10^6 cells per 10 cm tissue culture dish in the presence of 5 μM RA on the day of induction. The cells were grown for 7 days with substituting for culture medium with RA every other day. Total cellular RNA for preparing the RT–PCR templates was extracted after culturing for 7 days.

Cell cycle analysis

Approximately 50–70% confluent of HeLa cells were treated each by 400 μM mimosine for 18 h (G1 arrest), 2 mM thymidine for 20 h (S arrest), and 0.6 μg/ml nocodazole for 18 h (G2/M arrest). After confirmation of a synchronization of cultured cells by FACS, total RNA was extracted and the expression of *BMCC1* was examined by RT–PCR.

Northern blot analysis

Total RNA (25 μg) prepared from cell lines was electrophorased in 1% agarose-formaldehyde gels and transferred to a nylon membrane. For the hybridization probe, 1.5 kb fragment in 3′ part of *BMCC1* was used. Hybridization and washing were performed as described previously (Nagai *et al*., 2000).

Transfection and antibodies

Cells at 90% confluence in 60-mm plates were transfected with indicated plasmids using FuGENE 6 transfection reagent (Roche) for COS-7 and Lipofectamine 2000 reagent (Invitrogen) for HEK 293 cells according to their manufacturer's instructions. To generate the BMCC-1-specific antibody, rabbit antiserum was raised against the peptides individually (residues 31–59, 836–858, 993–1022, 1378–1402, 1719–1737, 2180–2209, 2693–2714) of human BMCC1. The antibody specific to C-terminal end of BMCC1 is crossreacted to human (transfectants), mouse (Neuro 2A) and rat (PC12) BMCC-1. Antiactin IgG (polyclonal) was purchased from Sigma, St Louis, MO, USA.

Semiquantitative RT–PCR

For semiquantitative RT–PCR analysis, 5 μg of total RNAs were converted to cDNA using random primers by Superscript II reverse transcriptase (Gibco-BRL). In all, 2 μl of the 100-fold dilution of cDNA was subjected to PCR. The 20 μl of PCR reaction mixture contained 1 μM forward and reverse primer specific for *BMCC1*, 250 μM deoxynucleotide triphosphates (dNTPs), 50 mM KCl, 10 mM Tris-HCl (pH 8.0), 1.5 mM $MgCl_2$ and 0.5 U Taq DNA polymerase (TAKARA, Otsu, Japan). The PCR amplification was carried out for 35 cycles (preheat at 95°C for 2 min, denature at 95°C for 15 s, annealing at 58°C for 15 s, and extension at 72°C for 20 s) in thermocycler (Perkin-Elmer Cetus, Foster City, CA, USA). The PCR products were electrophorased in 2.5% agarose gel, and visualized by UV illuminator. *BMCC1* primer sequences were as follows; forward: 5′-CGTTTATTTGCCGGTAGG AG-3′, reverse: 5′-GCTCAGGCTCTTTGGTAGGA-3′. As a control, *GAPDH* primers (forward primer; 5′-CTGCACCAA CAATATCCC-3′, reverse primer; 5′-GTAGAGACAGGG TTTCAC-3′) were also used with reduced cycle (28 cycles).

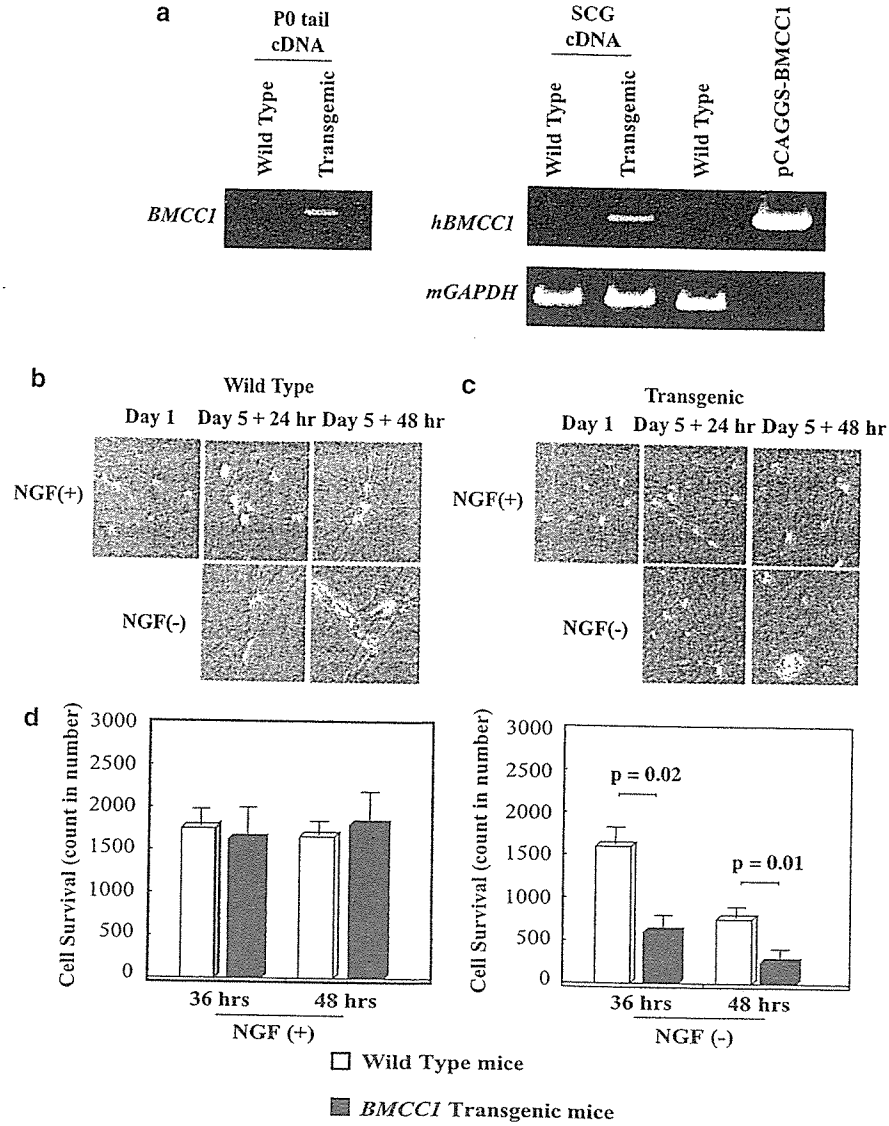

Figure 6 Increased apoptosis in superior cervical neurons obtained from newborn mice transgenic with the tyrosine hydroxylase promoter-driven human *BMCC1* in primary culture. (a) Expression of human *BMCC1* in SCG neurons obtained from *BMCC1* transgenic mice. SCG from both side of submandibular region was dissected from P_1 mice of wild-type and transgenic mice within 24 h after birth (described in Materials and methods). mRNA was purified from SCGs by using Trizol solution and RT–PCR was performed to confirm BMCC1 expression. Genotyping by PCR is shown in left panel. (b) and (c) Morphological changes in SCG neurons after treating with NGF and withdrawal of NGF. The SCG cells were obtained from wild-type (b) and BMCC1 transgenic (c) newborn mice. The cells were cultured in the presence of 50 ng/ml NGF for 5 days and were continuously treated with or without 50 ng/ml NGF for the following 2 days as described in Materials and methods. (d) Enhanced apoptosis in *BMCC1* transgenic SCG neurons after depletion of NGF. Numbers of survived SCG cells were counted at 36 and 48 h after NGF depletion. Values are shown as the means ± s.e.m. from triplicate cultures. Similar results were obtained in two additional independent experiments.

Quantitative real-time PCR analysis

For quantification of *BMCC1* in primary NBL, cDNA was synthesized with random primers by Superscript II reverse transcriptase (Gibco-BRL) from 15 μg of primary tumor total RNA. The following primers and probe were used; forward primer 5′-GGACAGTGGTCATTGGAGAACA-3′, reverse primer 5′-TTAGACCGTCCCCATAGTATCCTC-3′, probe 5′-FAM-ACATGAAGGTCATCGAGCCCTACAGG AGAG-TAMRA-3′. *GAPDH* primers and probes for control were purchased from Applied Biosystems. Quantitative real-time PCR analysis was performed by ABI7700 Prism sequence detector (Applied Biosystems), according to manufacturer's instructions using 1 × TaqMan Universal PCR Master Mix. After denaturing at 95°C for 10 min, PCR amplification followed by 40 cycles of denaturation at 95°C for 15 s and annealing/extension at 60°C for 1 min. A quantification of *BMCC1* mRNA in each samples was carried out by comparing with a standard curve, which was generated by reacting the plasmid containing *BMCC1*. Furthermore, *GAPDH* mRNA quantification was also performed for a standardization of the initial RNA content of each samples.

Exon prediction and bioinformatics

BLAST search against genome database revealed that 5′-region of *Nbla00219* was matched to the genome sequence of a

BAC clone RP11-146P9 (GenBank accession no. AL161625). We used GENESCAN algorithm (Burge and Karlin, 1997, 1998), and FGENESH algorithm (Solovyev and Salamov, 1999) to predict ORF from the genome sequence, and designed primers from each deduced exons. Using these primers and primers from 5′-region of *Nbla00219* cDNA, RT–PCR was performed to confirm the real exons. All PCR products were sequenced by the ABI automatic DNA sequencer (Perkin-Elmer Cetus) and resulting sequence were assembled to the full-length *BMCC1* cDNA. Bioinformatic analysis was performed using the PSORTII algorithm (Horton and Nakai, 1996), the SOPM algorithm and the TM pred algorithm against the predicted amino-acid sequences of *BMCC1*.

In situ *hybridization*
Section *in situ* hybridization was carried out as described previously (Takihara *et al*., 1997). The embryos were collected from pregnant females, and the morning the vaginal plug was detected was recorded as E0.5. A riboprobe was synthesized with digoxygenin-UTP and T3 or T7 polymerase (Roche Molecular Biochemicals). The alkaline phosphatase reaction was performed with NBT-BCIP (Roche Molecular Biochemicals). The riboprobes used for the section *in situ* hybridization were transcripts of the genomic DNA fragments of the *BMCC1* gene, a 835 bp PCR product of exon 3: the primers used are 5′-GAGATACTGGAGTTAGAAGAAG-3′ and 5′-TTCGGTCTTGGCTTTCTGGGTC-3′.

Immunohistochemistry
NBLs of favorable histology (Shimada system) without *MYCN* amplification and those of unfavorable histology with *MYCN* amplification were analysed. Anti-BMCC1 antibody was diluted to 1:50 and applied to the immunostaining. After deparaffinization, the sections were treated with 0.05% pronase solution for 5 min at room temperature. The biotin–streptoavidin method (Nichirei, Tokyo, Japan) was performed, and the reaction was visualized with diaminobenzidine solution.

Generation of BMCC1 transgenic mice
The full-length cDNA encoding human *BMCC1* was subcloned into the *Eco*RI site of the multicloning site region of the transgenic expression vector pCAGGS. The resulting plasmid, pCAGGS-*BMCC1*, was digested by *Alw44*I to isolate the transgenic cassette consisting of the CMV enhancer, the chicken *β-actin* promoter, the *BMCC1* cDNA, and the rabbit *β-globin* poly(A) sequence. The isolated region was purified for pronuclear injection into mouse embryos from FVB mice (Charles River Japan Inc.). Mouse embryos (fertilized one-cell zygotes) were injected and implanted in female CD-1 mice (Charles River Japan Inc.) at Japan SLC Inc. (Shizuoka, Japan). *BMCC1* transgenic mice were identified by slot blot analysis using genomic DNA prepared from mouse tails. *BMCC1*-positive founder transgenic mice then were backcrossed at least three times with C57BL/6 mice. Positive mice comprising the F_4 generation were subjected to SCG analyses.

Primary culture of newborn mice SCG cells
Primary cultures of sympathetic neurons were generated from dissociated SCG of postnatal-day 1 wild-type and transgenic mice as described previously (Lee *et al*., 1980). The cells were plated onto collagen-coated 24-well dishes at a density of around two ganglia per well and maintained in Modified Eagle's Medium supplemented with 10% heat-inactivated donor serum and 50 ng of mouse NGF per ml. A mixture of uridine and 5-fluorodeoxyuridine (10 μM each) was added on the following day to eliminate non-neuronal cells.

Statistical analysis
The Student's *t*-tests were used to explore possible associations between *BMCC1* expression and other factors, such as age. Since the values of the *BMCC1* expression were skewed, a log transformation was used to achieve the normality when using *t*-test and Cox regression. The distinction between high and low levels of *BMCC1* was based on the median value of the real-time PCR data (low, *BMCC1* <0.86 d.u.; high, *BMCC1* $\geqslant 0.86$ d.u.), regardless of tumor stage, *MYCN* copy, or survival. Kaplan–Meier survival curves were calculated, and survival distributions were compared using the log-rank test. Cox regression models were used to explore associations between *BMCC1*, age, *MYCN*, MS, origin and survival. Statistical significance was declared if the *P*-value was <0.05. Statistical analysis was performed using Stata 6.0. (Stata Corp. 1998. Stata Statistical Software: Release 6.0 College Station, TX: Stata Corporation).

Acknowledgements

We thank Shigeyuki Furuta, Shiho Hamano, Hiroyuki Inuzuka, Aiko Morohashi for technical assistance, Masayuki Fukumura, Toshihide Kanamori and Mika Kimura for helping full-length cDNA cloning, and Shigeru Sakiyama for encouragement. This work was supported in part by a Grant-in-Aid for the 2nd Term Comprehensive 10-Year Strategy for Cancer Control from the Ministry of Health, Labour and Welfare of Japan (AN), and by Grant-in-Aid for Scientific Research (B) (AN) and for Scientific Research on Priority Areas (2) 'Medical Genome Science' (MO, EI, AN) from the Ministry of Education, Culture, Sports, Science and Technology of Japan, and by a fund from Hisamitsu Pharmaceutical Co. Inc. (AN). We also thank following hospitals and departments for providing surgical samples: First Department of Surgery, Hokkaido University School of Medicine; Department of Pediatrics, National Sapporo Hospital; Department of Pediatric Surgery, Tohoku University School of Medicine; Department of Surgery, Gunma Children's Medical Center; Department of Pediatrics, Pediatric Surgery and General Surgery, Jichi Medical University; Department of Hematology and Oncology, Saitama Children's Medical Center; Department of Pediatrics, Juntendo University School of Medicine; Department of Surgery, Kiyose Metropolitan Children's Hospital; Department of Surgery and Pathology, Chiba Children's Hospital; Department of Pediatric Surgery, Chiba University School of Medicine; Department of Pediatric Surgery, Kimitsu Central Hospital; Department of Pediatric Surgery, Niigata University School of Medicine; Department of Pediatrics and Pediatric Surgery, Aichi Medical University; Department of Pediatrics, Kyoto Prefectural Medical University; Tumor Board, Hyogo Children's Hospital; Department of Pediatrics and Pediatric Surgery, Kagoshima University School of Medicine; Department of Pediatric Surgery, Showa University School of Medicine; Department of Pediatrics, Oita University School of Medicine; Department of Pediatric Surgery, Ohta General Hospital; Department of Pediatrics, Ichinomiya City Hospital; Department of Pediatric Surgery, Osaka City General Hospital; Department of Pediatrics, Nihon University School of Medicine Itabashi Hospital; Department of Pediatric Surgery, University of Tsukuba School of Medicine.

References

Bagrodia S, Derijard B, Davis RJ, Cerione RA. (1995). *J Biol Chem* **270**: 27995–27998.
Bazenet CE, Mota MA, Rubin LL. (1998). *Proc Natl Acad Sci USA* **95**: 3984–3989.
Boyd JM, Malstrom S, Subramanian T, Venkatesh LK, Schaeper U, Elangovan B *et al.* (1994). *Cell* **79**: 341–351.
Brodeur GM, Pritchard J, Berthold F, Carlsen NL, Castel V, Castelberry RP *et al.* (1993). *J Clin Oncol* **11**: 1466–1477.
Brodeur GM, Seeger RC, Schwab M, Varmus HE, Bishop JM. (1984). *Science* **224**: 1121–1124.
Burge C, Karlin S. (1997). *J Mol Biol* **268**: 78–94.
Burge CB, Karlin S. (1998). *Curr Opin Struct Biol* **8**: 346–354.
Cahill MA, Peter ME, Kischkel FC, Chinnaiyan AM, Dixit VM, Krammer PH *et al.* (1996). *Oncogene* **13**: 2087–2096.
Caron H. (1995). *Med Pediatr Oncol* **24**: 215–221.
Chuang TH, Hahn KM, Lee JD, Danley DE, Bokoch GM. (1997). *Mol Biol Cell* **8**: 1687–1698.
Coso OA, Chiariello M, Yu JC, Teramoto H, Crespo P, Xu N *et al.* (1995). *Cell* **81**: 1137–1146.
Evans AE, Gerson J, Schnaufer L. (1976). *Natl Cancer Inst Monogr* **44**: 49–54.
Favrot MC, Combaret V, Lasset C. (1993). *N Engl J Med* **329**: 1965.
Garcia I, Martinou I, Tsujimoto Y, Martinou JC. (1992). *Science* **258**: 302–304.
Garnier M, Di Lorenzo D, Albertini A, Maggi A. (1997). *J Neurosci* **17**: 4591–4599.
Gjoerup O, Lukas J, Bartek J, Willumsen BM. (1998). *J Biol Chem* **273**: 18812–18818.
Gooding LR, Aquino L, Duerksen-Hughes PJ, Day D, Horton TM, Yei SP *et al.* (1991). *J Virol* **65**: 3083–3094.
Hashimoto S, Ishii A, Yonehara S. (1991). *Int Immunol* **3**: 343–351.
Hockenbery D, Nunez G, Milliman C, Schreiber RD, Korsmeyer SJ. (1990). *Nature* **348**: 334–336.
Horton P, Nakai K. (1996). *Proc Int Conf Intell Syst Mol Biol* **4**: 109–115.
Islam A, Kageyama H, Takada N, Kawamoto T, Takayasu H, Isogai E *et al.* (2000). *Oncogene* **19**: 617–623.
Juo P, Kuo CJ, Reynolds SE, Konz RF, Raingeaud J, Davis RJ *et al.* (1997). *Mol Cell Biol* **17**: 24–35.
Kaneko M, Nishihira H, Mugishima H, Ohnuma N, Nakada K, Kawa K *et al.* (1998). *Med Pediatr Oncol* **31**: 1–7.
Kozak M. (1987). *Nucl Acids Res* **15**: 8125–8148.
Larisch S, Yi Y, Lotan R, Kerner H, Eimerl S, Tony Parks W *et al.* (2000). *Nat Cell Biol* **2**: 915–921.
Lee VM, Shelanski ML, Greene LA. (1980). *Neuroscience* **5**: 2239–2245.
Lenczowski JM, Dominguez L, Eder AM, King LB, Zacharchuk CM, Ashwell JD. (1997). *Mol Cell Biol* **17**: 170–181.
Low BC, Seow KT, Guy GR. (2000). *J Biol Chem* **275**: 37742–37751.
Moasser MM, Khoo KS, Maerz WJ, Zelenetz A, Dmitrovsky E. (1996). *Differentiation* **60**: 251–257.
Nagai M, Ichimiya S, Ozaki T, Seki N, Mihara M, Furuta S *et al.* (2000). *Int J Oncol* **16**: 907–916.
Nakagawara A. (1998). *Hum Cell* **11**: 115–124.
Nakagawara A. (2001). *Cancer Lett* **169**: 107–114.
Nakagawara A, Arima-Nakagawara M, Scavarda NJ, Azar CG, Cantor AB, Brodeur GM. (1993). *N Engl J Med* **328**: 847–854.
Nakagawara A, Azar CG, Scavarda NJ, Brodeur GM. (1994). *Mol Cell Biol* **14**: 759–767.
Nakagawara A, Milbrandt J, Muramatsu T, Deuel TF, Zhao H, Cnaan A *et al.* (1995). *Cancer Res* **55**: 1792–1797.
Nakamura Y, Ozaki T, Ichimiya S, Nakagawara A, Sakiyama S. (1998). *Biochem Biophys Res Commun* **243**: 722–726.
Ohira M, Morohashi A, Inuzuka H, Shishikura T, Kawamoto T, Kageyama H *et al.* (2003a). *Oncogene* **22**: 5525–5536.
Ohira M, Morohashi A, Nakamura Y, Isogai E, Furuya K, Hamano S *et al.* (2003b). *Cancer Lett* **197**: 63–68.
Olson MF, Ashworth A, Hall A. (1995). *Science* **269**: 1270–1272.
Oltvai ZN, Milliman CL, Korsmeyer SJ. (1993). *Cell* **74**: 609–619.
Seimiya H, Mashima T, Toho M, Tsuruo T. (1997). *J Biol Chem* **272**: 4631–4636.
Shimada H, Chatten J, Newton Jr WA, Sachs N, Hamoudi AB, Chiba T *et al.* (1984). *J Natl Cancer Inst* **73**: 405–416.
Solovyev VV, Salamov AA. (1999). *Nucl Acids Res* **27**: 248–250.
Subramanian T, Boyd JM, Chinnadurai G. (1995). *Oncogene* **11**: 2403–2409.
Takihara Y, Tomotsune D, Shirai M, Katoh-Fukui Y, Nishii K, Motaleb MA *et al.* (1997). *Development* **124**: 3673–3682.
Tanaka T, Sugimoto T, Sawada T. (1998). *Cancer* **83**: 1626–1633.
Vegeto E, Pollio G, Pellicciari C, Maggi A. (1999). *FASEB J* **13**: 793–803.
White E, Sabbatini P, Debbas M, Wold WS, Kusher DI, Gooding LR. (1992). *Mol Cell Biol* **12**: 2570–2580.
Whitfield J, Neame SJ, Paquet L, Bernard O, Ham J. (2001). *Neuron* **29**: 629–643.
Yamamoto M, Marui N, Sakai T, Morii N, Kozaki S, Ikai K *et al.* (1993). *Oncogene* **8**: 1449–1455.
Yuan J, Horvitz HR. (1992). *Development* **116**: 309–320.
Zhang B, Zhang Y, Collins CC, Johnson DI, Zheng Y. (1999). *J Biol Chem* **274**: 2609–2612.
Zhang B, Zheng Y. (1998). *J Biol Chem* **273**: 25728–25733.
Zhang S, Han J, Sells MA, Chernoff J, Knaus UG, Ulevitch RJ *et al.* (1995). *J Biol Chem* **270**: 23934–23936.
Zhou YT, Soh UJ, Shang X, Guy GR, Low BC. (2002). *J Biol Chem* **277**: 7483–7492.
Zou H, Henzel WJ, Liu X, Lutschg A, Wang X. (1997). *Cell* **90**: 405–413.

Oncogene (2006) 25, 5046–5055

www.nature.com/onc

ORIGINAL ARTICLE

Bcl-2 is a key regulator for the retinoic acid-induced apoptotic cell death in neuroblastoma

H Niizuma[1,2], Y Nakamura[1], T Ozaki[1], H Nakanishi[1], M Ohira[1], E Isogai[1], H Kageyama[1], M Imaizumi[3] and A Nakagawara[1]

[1]Division of Biochemistry, Chiba Cancer Center Research Institute, Chuoh-ku, Chiba, Japan; [2]Department of Pediatrics, Tohoku University School of Medicine, Aoba-ku, Sendai, Japan and [3]Department of Hematology and Oncology, Miyagi Children's Hospital, Aoba-ku, Sendai, Japan

Retinoic acid (RA) has been shown to induce neuronal differentiation and/or apoptosis, and is widely used as a chemotherapeutic agent for treating the patients with neuroblastoma. However, the therapeutic effect of RA is still limited. To unveil the molecular mechanism(s) inducing differentiation and apoptosis in neuroblastoma cells, we compared CHP134 and NB-39-nu cell lines, in which all-*trans*-RA (ATRA) induces apoptosis, with LA-N-5 and RTBM1 cell lines, in which it induces neuronal differentiation. Here, we found that Bcl-2 was strongly downregulated in CHP134 and NB-39-nu cells, whereas it was abundantly expressed in LA-N-5 and RTBM1 cells. ATRA-mediated apoptosis in CHP134 and NB-39-nu cells was associated with a significant activation of caspase-9 and caspase-3 as well as cytoplasmic release of cytochrome *c* from mitochondria in a p53-independent manner. Enforced expression of Bcl-2 significantly inhibited ATRA-mediated apoptosis in CHP134 cells. In addition, treatment of RTBM1 cells with a Bcl-2 inhibitor, HA14-1, enhanced apoptotic response induced by ATRA. Of note, two out of 10 sporadic neuroblastomas expressed *bcl-2* at undetectable levels and underwent cell death in response to ATRA in primary cultures. Thus, our present results suggest that overexpression of Bcl-2 is one of the key mechanisms to give neuroblastoma cells the resistance against ATRA-mediated apoptosis. This may provide a new therapeutic strategy against the ATRA-resistant and aggressive neuroblastomas by combining treatment with ATRA and a Bcl-2 inhibitor.
Oncogene (2006) **25**, 5046–5055. doi:10.1038/sj.onc.1209515; published online 27 March 2006

Keywords: apoptosis; Bcl-2; neuroblastoma; retinoic acid

Correspondence: Dr A Nakagawara, Division of Biochemistry, Chiba Cancer Center Research Institute, 666-2 Nitona, Chuoh-ku, Chiba 260-8717, Japan.
E-mail: akiranak@chiba-cc.jp
Received 8 November 2005; revised 6 February 2006; accepted 15 February 2006; published online 27 March 2006

Introduction

Neuroblastoma, which originates from the sympathoadrenal lineage of the neural crest, is one of the most common solid tumors in childhood and has distinct biological properties in different prognostic subsets (Schor, 1999). For example, tumors in patients less than 1 year of age often regress spontaneously and have a favorable prognosis. In contrast, tumors that occur over 1 year of age display an extensive and metastatic disease at diagnosis, and are often aggressive with an unfavorable prognosis despite an intensive therapy (Brodeur and Nakagawara, 1992). Each of those subsets shows various distinct genetic features including the ploidy status, *MYCN* amplification, allelic loss of the distal part of chromosome 1p and the gain of chromosome 17q (Brodeur, 2003). Additionally, high expression levels of neurotrophin receptors TrkA and TrkB are favorable and unfavorable prognostic indicators of neuroblastomas, respectively (Nakagawara *et al.*, 1993, 1994). Several lines of evidence suggest that the spontaneous regression of the favorable neuroblastomas is attributed at least in part to the developmentally programmed neuronal cell death and/or neuronal differentiation (Nakagawara, 1998). Indeed, the deprivation of nerve growth factor led to the massive cell death through apoptosis of neuroblastoma cells expressing TrkA (Nakagawara *et al.*, 1993).

Retinoic acids (RAs), which appear to be involved in vertebrate morphogenesis, are natural and synthetic derivatives of vitamin A (Maden, 2001; McCaffery *et al.*, 2003), and exert their biological functions through nuclear receptors including RA receptors (RARs) and retinoid X receptors (RXRs) (Lippman and Lotan, 2000). In response to RA binding, RAR/RXR heterodimers regulate the transcription of a number of target genes by binding to the specific DNA response elements (Balmer and Blomhoff, 2002). Retinoic acids have antitumor effects on neuroblastoma-derived cell lines accompanied by a marked decrease in the expression levels of *MYCN* (Thiele *et al.*, 1985). Studies utilizing cell lines also have revealed that neuroblastoma cell lines exposed to all-*trans*-RA (ATRA) undergo neuronal differentiation, cell cycle arrest and/or apoptosis (Melino *et al.*, 1997; van Noesel and Versteeg, 2004). Recent

works offer insights into the molecular mechanisms by which ATRA exerts its biological effects on neuroblastomas. All-*trans*-retinoic acid activates phosphatidylinositol 3′-kinase-Akt pathway that plays an important role in neuronal differentiation (Encinas *et al.*, 1999; Lopez-Carballo *et al.*, 2002), and it reduces the expression levels of MYCN (Thiele *et al.*, 1985) and upregulates the cyclin-dependent kinase (CDK) inhibitor $p27^{KIP1}$ in association with the ATRA-induced cell cycle arrest in neuroblastoma cells (Lee *et al.*, 1996; Nakamura *et al.*, 2003). In addition, certain neuroblastoma cells underwent apoptosis in response to ATRA (Piacentini *et al.*, 1992; Takada *et al.*, 2001; Nagai *et al.*, 2004). Consistent with these observations, 13-*cis*-RA treatment after intensive chemotherapy improved an event-free survival rate of the patients with aggressive neuroblastomas with 17% increase (Villablanca *et al.*, 1995; Matthay *et al.*, 1999). Although the antitumor effects of RA alone on aggressive neuroblastoma are limited, RA treatment has an advantage that it carries no severe side effects. Thus, it is important to enhance the antitumor effects of RA on neuroblastoma cells, and thereby inducing apoptosis.

In the present study, we have found that the ATRA treatment induces neuronal differentiation in neuroblastoma-derived LA-N-5 and RTBM1 cells, whereas CHP134 and NB-39-nu cells undergo p53-independent apoptotic cell death in response to ATRA. Extensive expression studies revealed that the antiapoptotic Bcl-2 was constitutively expressed at high levels in LA-N-5 and RTBM1 cells, whereas CHP134 and NB-39-nu cells expressed Bcl-2 at extremely low levels. Enforced expression of Bcl-2 in CHP134 cells led to a significant inhibition of the ATRA-mediated apoptosis. In accordance with these results, the treatment with Bcl-2 inhibitor in RTBM1 cells resulted in an increased sensitivity to ATRA. Moreover, two out of 10 sporadic neuroblastomas in primary cultures with undetectable *bcl-2* underwent cell death in response to ATRA, whereas seven tumors out of the remaining eight cases expressed high levels of *bcl-2*. These results suggest that Bcl-2 might be a key regulator for the ATRA-mediated apoptotic cell death in neuroblastomas.

Results

ATRA-induced growth inhibition, differentiation and cell death in human neuroblastoma cell lines

To examine the possible effects of ATRA on growth and viability of neuroblastoma cells, human neuroblastoma-derived LA-N-5, RTBM1, CHP134 and NB-39-nu cells were cultured with or without 5 μM of ATRA, and the numbers of viable cells were counted at the indicated time points after the exposure to ATRA. As shown in Figure 1a, ATRA effectively inhibited proliferation of these neuroblastoma cells. Among them, the growth of CHP134 and NB-39-nu cells was much more suppressed in the presence of ATRA. To monitor morphological changes induced by ATRA, ATRA-treated cells were checked by phase-contrast microscopy. As shown in Figure 1b, a neurite outgrowth was evident in ATRA-treated LA-N-5, RTBM1 and CHP134 cells, whereas it was marginal in NB-39-nu cells. Of note, ATRA-induced cell death was detectable in CHP134 and NB-39-nu cells, but not in LA-N-5 and RTBM1 cells. To confirm whether ATRA could induce the apoptotic cell death in CHP134 and NB-39-nu cells, we examined the changes in the number of cells with sub-G1 DNA content in response to ATRA. As shown in Figure 1c and d, the flow cytometric analysis revealed that the number of CHP134 cells with sub-G1 DNA content was significantly increased in response to ATRA. Similarly, ATRA promoted the apoptotic cell death in NB-39-nu cells, albeit to a lesser degree than CHP134 cells. Under our experimental conditions, ATRA failed to induce the apoptotic cell death in LA-N-5 and RTBM1 cells (data not shown).

ATRA-induced apoptotic cell death in neuroblastoma cells

To elucidate the molecular mechanism(s) underlying the ATRA-mediated apoptotic cell death in neuroblastoma cells, we examined whether the procaspases could be proteolytically cleaved to be activated in response to ATRA. To this end, whole-cell lysates prepared from the indicated neuroblastoma cells exposed to 5 μM of ATRA for 0, 2, 4 and 6 days were subjected to immunoblotting with the indicated antibodies. As shown in Figure 2a, the time-dependent proteolytic cleavage of caspase-9 and caspase-3 was observed in CHP134 and NB-39-nu cells, but not in LA-N-5 and RTBM1 cells. Consistent with these results, one of the physiological substrates of the activated caspase-3, poly-ADP-ribose polymerase (PARP), was cleaved in ATRA-treated CHP134 and NB-39-nu cells. In a good agreement with the previous observations showing that caspase-8 is epigenetically silenced in a high percentage of neuroblastoma cells (Teitz *et al.*, 2000; van Noesel *et al.*, 2003), caspase-8 was undetectable in LA-N-5, RTBM1 and CHP134 cells. In contrast, NB-39-nu cells expressed a large amount of procaspase-8. Procaspase-12, which is involved in the endoplasmic reticulum-stress-induced apoptosis (Nakagawa *et al.*, 2000; Morishima *et al.*, 2002), was readily detectable in all of the neuroblastoma cell lines that we examined, and did not respond to ATRA. Under our experimental conditions, ATRA had negligible effects on proteolytic cleavage of caspase-8 and caspase-12 (data not shown).

As caspase-9 is activated in response to the cytoplasmic release of cytochrome *c* from mitochondria, leading to the activation of caspase-3 (Degterev *et al.*, 2003), we sought to examine whether cytochrome *c* could be released in response to ATRA. To this end, CHP134 cells were treated with 5 μM of ATRA or left untreated, and cells were incubated with the antibody against cytochrome *c* or with the control immunoglobulin (Ig)G. Cell nuclei were stained with 4,6-diamidino-2-phenylindole (DAPI). Microscopic images demonstrated that cytochrome *c* staining displays a punctuate

cytoplasmic pattern in the absence of ATRA (Figure 2b, left). This staining pattern was almost identical to the MitoTracker staining (data not shown). ATRA treatment for 4 days induced redistribution of cytochrome *c* to a diffused cytoplasmic pattern in cells with apoptotic nuclei (Figure 2b, middle), suggesting

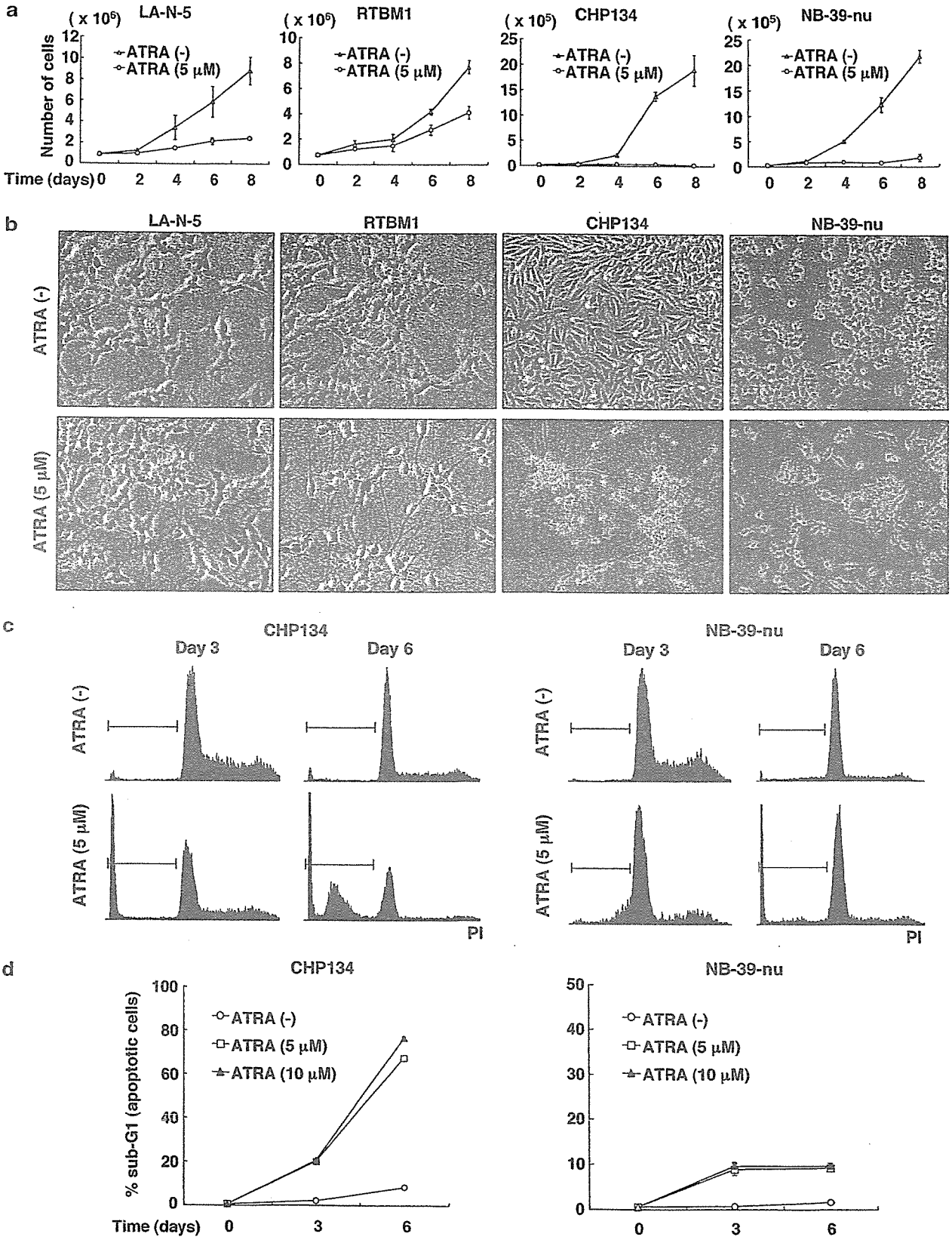

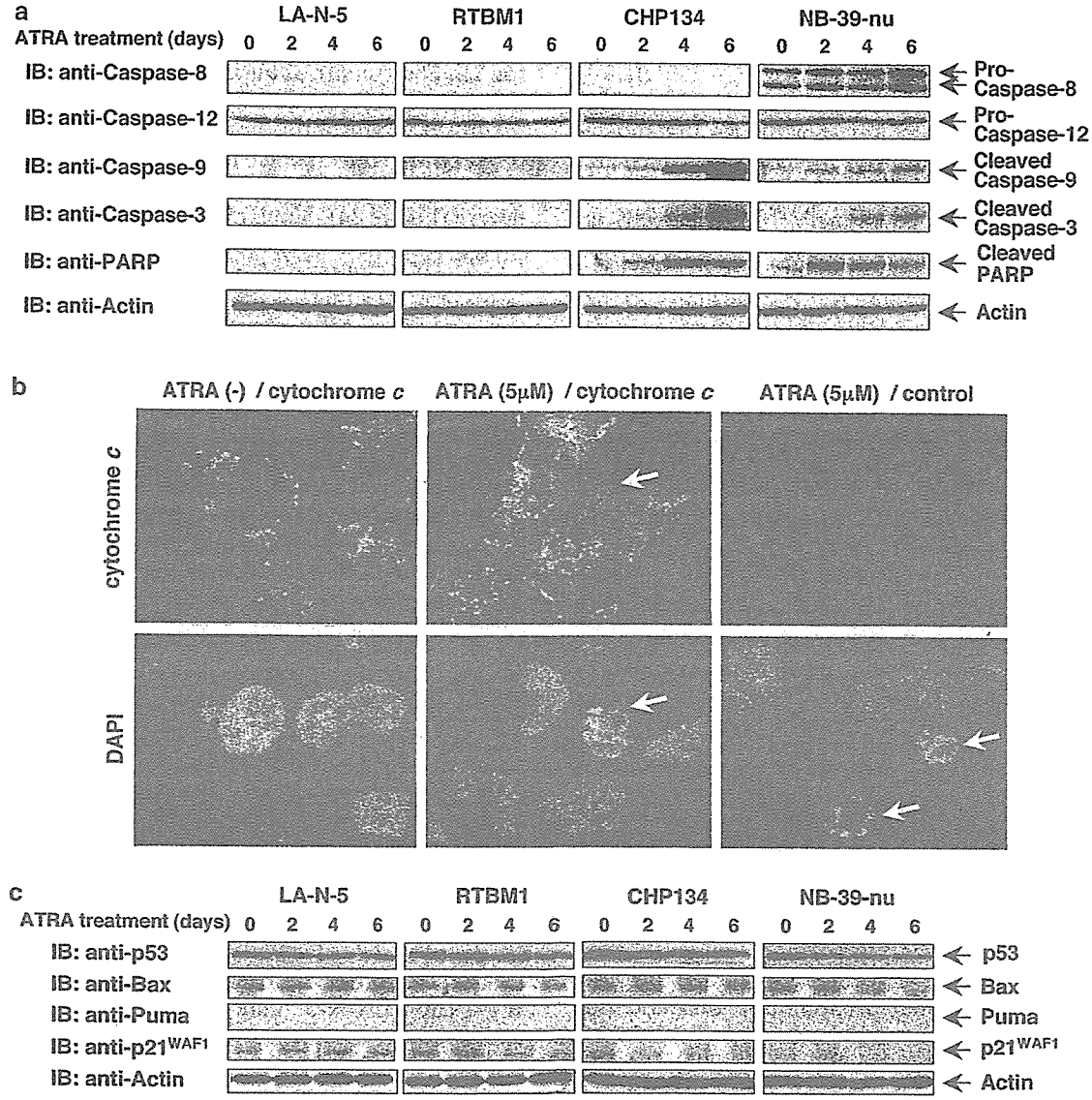

Figure 2 Caspase-9 and caspase-3 are cleaved during the all-*trans* retinoic acid (ATRA)-mediated apoptosis in CHP134 and NB-39-nu cells. (a) Immunoblot analysis for various caspases and poly-ADP-ribose polymerase (PARP) in response to ATRA. The indicated neuroblastoma cell lines were treated with 5 μM of ATRA or left untreated. At the indicated time points after the treatment with ATRA, whole-cell lysates were prepared, and analysed by immunoblotting with indicated antibodies. Actin expression was used as a loading control (bottom). (b) ATRA-induced cytoplasmic release of cytochrome *c* in CHP134 cells. CHP134 cells were seeded onto coverslips, and cultured in the presence or absence of 5 μM of ATRA. Four days after the treatment with ATRA, cells were fixed and stained with a monoclonal antibody against cytochrome *c* (top, left and middle) or with a normal mouse IgG (top, right). The cell nuclei were stained with 4,6-diamidino-2-phenylindole (DAPI) (bottom). The arrows indicate apoptotic cells with condensed and fragmented nuclei. (c) Expression levels of p53 and its direct target gene products in response to ATRA. At the indicated time periods after the treatment with ATRA, whole-cell lysates were prepared, and subjected to immunoblotting with antibodies against p53, Bax, Puma, $p21^{WAF1}$ and actin. Immunoblotting for actin is shown as a control for protein loading (bottom).

Figure 1 Effects of all-*trans* retinoic acid (ATRA) on cell proliferation of LA-N-5, RTBM1, CHP134 and NB-39-nu neuroblastoma-derived cell lines. (a) Growth curves of the indicated neuroblastoma cell lines in the presence or absence of ATRA. Cells were grown in the standard culture medium, and treated with 5 μM of ATRA. At the indicated time points after the treatment with ATRA, cells were trypsinized, harvested and number of viable cells was counted in triplicate. (b) ATRA-induced morphological changes of neuroblastoma cell lines. Cells were exposed to ATRA at a final concentration of 5 μM or left untreated. Six days after the treatment with ATRA, cells were examined by phase-contrast microscopy. (c and d) ATRA-induced cell death through apoptosis in CHP134 and NB-39-nu cells. Cells were treated with the indicated concentrations of ATRA or left untreated, and incubated for up to 6 days. At the indicated time points after the treatment with ATRA, cells were collected, fixed and stained with propidium iodide (PI). The DNA content of the cells was then examined by flow cytometry (c). The number of cells with sub-G1 DNA content was counted in triplicate (d).

that cytochrome *c* release from mitochondria might play an important role in ATRA-induced apoptotic cell death in neuroblastoma cells.

As the neuroblastoma cell lines that we examined carry wild-type p53 (data not shown), we investigated whether p53 could contribute to the ATRA-mediated apoptotic cell death. For this purpose, whole-cell lysates prepared from the indicated neuroblastoma cells exposed to 5 μM of ATRA for 0, 2, 4 and 6 days were processed for immunoblotting with the indicated antibodies. As shown in Figure 2c, the amounts of p53 remained unchanged or slightly decreased after ATRA treatment. In accordance with these results, ATRA had undetectable effects on the expression levels of p53-responsible Bax, Puma and $p21^{WAF1}$, which are implicated in the p53-dependent apoptosis and/or cell cycle arrest (Culmsee and Mattson, 2005). In addition, ATRA failed to induce the phosphorylation of p53 at Ser-15 (data not shown). Thus, it is likely that ATRA-mediated apoptotic cell death in neuroblastoma cells may be regulated in a p53-independent manner.

Differential expression of antiapoptotic Bcl-2 in neuroblastoma cells

To investigate the regulatory mechanisms of apoptotic response to ATRA in neuroblastoma cells, we examined the expression levels of Bcl-2 family proteins, which directly control the mitochondrial pathway of apoptosis. It is worth noting that antiapoptotic Bcl-2 was constitutively expressed at high levels in LA-N-5 as well as RTBM1 cells, whereas CHP134 and NB-39-nu cells expressed Bcl-2 at extremely low levels (Figure 3a). Antiapoptotic Bcl-x_L was expressed at low levels in all cell lines examined. In accordance with the previous observations showing that proapoptotic Bim and Bmf are highly expressed in neuronal cells (Puthalakath *et al*., 2001; Okuno *et al*., 2004; Shi *et al*., 2004), Bim and Bmf were expressed at high levels in all of the cell lines that we examined, but their expression levels remained unchanged in the presence of ATRA.

To determine whether Bcl-2 could contribute to the acquisition of the ATRA-resistant phenotype of neuroblastoma cells, CHP134 cells were transfected with the expression plasmid for Bcl-2 or with the empty plasmid, and their sensitivity to ATRA was examined by flow cytometry. As shown in Figure 3b, Bcl-2 was successfully overexpressed in CHP134 cells as examined by immunoblotting. Interestingly, enforced expression of Bcl-2 inhibited the ATRA-mediated proteolytic cleavage of caspase-3. Consistent with these results, flow cytometric analysis demonstrated that ectopic expression of Bcl-2 significantly reduced the number of cells with sub-G1 DNA content induced by ATRA treatment (Figure 3c and d), suggesting that Bcl-2 might play a critical role in the regulation of apoptotic cell death in neuroblastoma cells.

To further confirm this possibility, we examined the effects of the Bcl-2 inhibitor HA14-1 (Wang *et al*., 2000) on the ATRA-mediated apoptotic response of neuroblastoma cells. RTBM1 cells were treated with 5 μM of ATRA or left untreated for 6 days, and then incubated in the presence or absence of HA14-1 (15, 30 or 50 μM) for 3 h. Phase-contrast microscopic analysis showed that the incubation with ATRA followed by HA14-1 treatment significantly enhanced the apoptotic response of RTBM1 cells, whereas HA14-1 treatment alone increased the number of apoptotic cells to a lesser degree (Figure 4a). Similar results were also obtained by flow cytometric analysis (Figure 4b and c). To examine whether the ATRA-mediated apoptosis in RTBM1 cells induced by HA14-1 treatment could be associated with the activation of the mitochondria-dependent apoptotic pathway, we performed immunoblot analysis. As shown in Figure 4d, HA14-1 treatment at 30 μM or less did not promote the activation of caspase-9 and caspase-3, whereas a small amount of the cleaved caspase-9 and caspase-3 were detectable in RTBM1 cells exposed to 50 μM of HA14-1 alone. Intriguingly, pre-treatment of RTBM1 cells with ATRA enhanced the proteolytic cleavage of caspase-9 and caspase-3 induced by HA14-1 at a final concentration of 50 μM.

To ask whether Bcl-2 could play an important role in ATRA-mediated apoptotic response in primary neuroblastomas, 10 sporadically found neuroblastomas were subjected to both primary culture and reverse transcriptase–polymerase chain reaction (RT-PCR) analysis for *bcl-2*. In five cases, ATRA treatment induced strong outgrowth of neurites as compared with control culture (Figure 5a, left). In the other three cases, ATRA had undetectable effects (data not shown). It is worth noting that many cells underwent cell death after ATRA treatment in the remaining two cases (Figure 5a, right). We also examined the expression levels of *bcl-2* of these 10 primary neuroblastoma samples and four neuroblastoma-derived cell lines by RT–PCR. LA-N-5 and RTBM1 cells abundantly expressed *bcl-2*, whereas CHP134 and NB-39-nu did not (Figure 5b), which was consistent with immunoblotting as shown in Figure 3a. Of particular interest, RT–PCR analysis revealed that two primary cases that underwent cell death in response to ATRA (N-9 and N-10) expressed *bcl-2* at undetectable levels (Figure 5c). In a sharp contrast, the expression of *bcl-2* was detected in the remaining cases, except N-3. Taken together, our present results strongly suggest that Bcl-2 is a key regulator for ATRA-mediated apoptotic cell death in neuroblastoma cells.

Discussion

Retinoic acid is one of the potent antitumor agents that has been used successfully to treat certain human tumors including neuroblastomas (Freemantle *et al*., 2003). Indeed, neuroblastoma patients treated with RA have increased survival rate without severe side effects (Villablanca *et al*., 1995; Matthay *et al*., 1999). Accumulating evidences suggest that RA plays an important role in the regulation of neuroblastoma apoptosis as well as differentiation (Melino *et al*.,

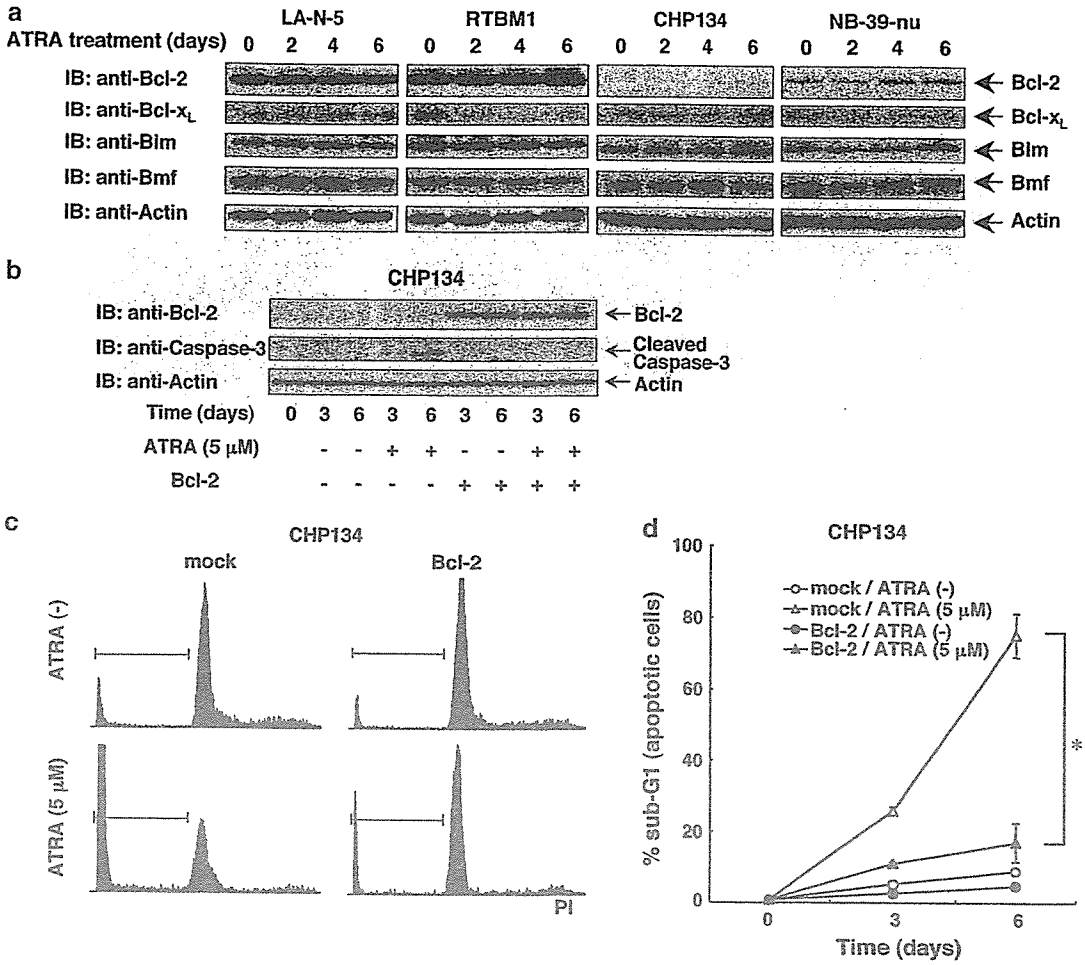

Figure 3 Differential expression of antiapoptotic Bcl-2 protein. (a) The indicated neuroblastoma cell lines were cultured in standard culture medium containing all-*trans* retinoic acid (ATRA) at a final concentration of 5 μM. At the indicated time points after the treatment with ATRA, whole-cell lysates were prepared, and analysed by immunoblotting with the antibodies against the indicated Bcl-2 family proteins. Actin expression was examined as a loading control (bottom). (b) Overexpression of Bcl-2. CHP134 cells were transiently transfected with the expression plasmid for Bcl-2 or with the empty plasmid. Twelve hours after the transfection, cells were treated with or without 5 μM ATRA, and incubated for additional 3 or 6 days. Whole-cell lysates were prepared, and the expression levels of Bcl-2 (top) and the amounts of the cleaved caspase-3 (middle) were examined by immunoblotting. Actin is shown as a control for protein loading (bottom). (c and d) Flow cytometry. CHP134 cells were transiently transfected as described in (b). At the indicated time periods after the treatment with ATRA, cells were collected, fixed and stained with PI. The DNA content of the cells was examined by flow cytometry. Representative results on day 6 are shown in (c). The number of cells with sub-G1 DNA content was counted in triplicate (d). *$P<0.01$.

1997; van Noesel and Versteeg, 2004). However, certain neuroblastomas display an RA-resistant phenotype (Reynolds and Lemons, 2001). To further improve the therapeutic effects of RA on neuroblastomas, it is necessary to clarify the detailed molecular mechanisms underlying the RA-mediated neuroblastoma differentiation and/or apoptosis. In the present study, we have found that ATRA causes growth suppression and subsequent neuronal differentiation in human neuroblastoma-derived LA-N-5, RTBM1, CHP134 and NB-39-nu cells to various degrees. Among them, CHP134 and NB-39-nu cells, which express antiapoptotic Bcl-2 at extremely low levels, underwent p53-independent apoptotic cell death in response to ATRA. In contrast, LA-N-5 and RTBM1 cells abundantly expressed Bcl-2, and we did not detect apoptotic cell death upon ATRA treatment. Enforced expression of Bcl-2 in CHP134 cells inhibited the ATRA-mediated apoptosis, and HA14-1-mediated inhibition of the endogenous Bcl-2 in RTBM1 cells enhanced the ATRA-dependent apoptotic cell death. Moreover, studies using primary neuroblastoma tissues showed that ATRA had toxic effect on two out of 10 primary cultures, and these ATRA-sensitive tumors did not express *bcl-2*. Thus, it is likely that antiapoptotic Bcl-2 plays a crucial role in the regulation of the ATRA-mediated apoptotic response in neuroblastomas.

Our present study revealed that neuroblastoma cells can be divided into two groups with respect to the ATRA-induced apoptotic response. CHP134 and NB-39-nu cells underwent apoptotic cell death in response to ATRA, whereas LA-N-5 and RTBM1 cells did not. Consistent with the mitochondria-dependent intrinsic apoptotic pathway of caspase activation (Degterev

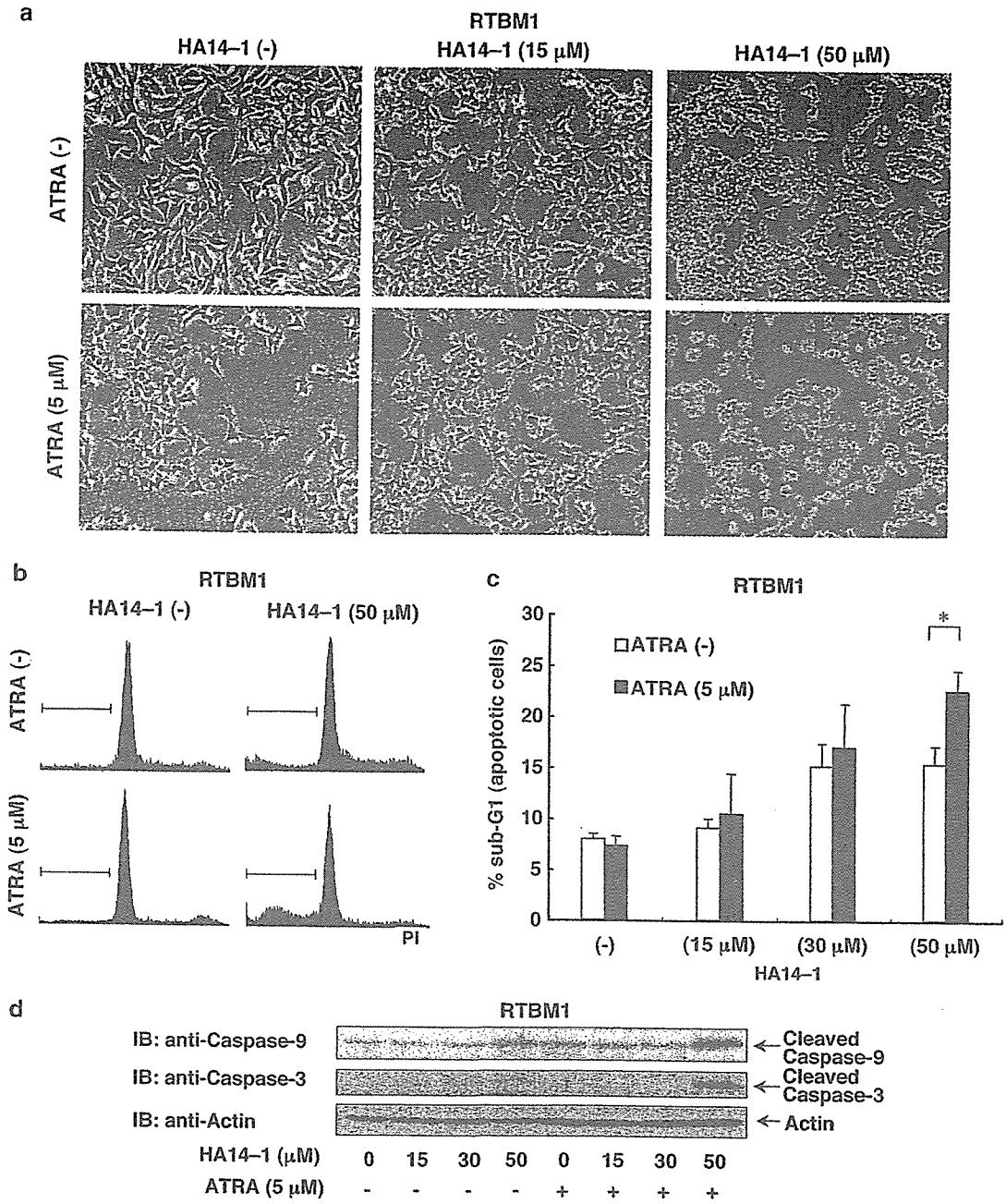

Figure 4 Bcl-2 inhibitor HA14-1 induces apoptosis of all-*trans* retinoic acid (ATRA)-treated RTBM1 cells. (**a**) Morphological changes after HA14-1 treatment of RTBM1 cells. RTBM1 cells were cultured with or without 5 μM ATRA for 6 days in advance, and then treated with HA14-1, a specific inhibitor of Bcl-2, at the indicated concentrations in standard medium for 3 h. Cells were examined by phase-contrast microscopy and photographed after the treatment. (**b** and **c**) FACS analysis. RTBM1 cells were treated with ATRA and HA14-1 as described in (**a**). Cells were collected, fixed and stained with PI. The DNA content of the cells was examined by flow cytometry and representative results are shown in (**b**). The number of cells with sub-G1 DNA content was counted in triplicate (**c**). $^*P<0.05$. (**d**) Immunoblotting. Whole-cell lysates of RTBM1 treated with ATRA and HA14-1 were prepared to examine the amounts of cleaved caspase-9 and caspase-3. Actin is shown as a loading control.

et al., 2003), ATRA treatment in CHP134 cells caused a cytoplasmic release of the mitochondrial inter-membrane protein cytochrome *c*, and a sequential proteolytic cleavage of caspase-9, caspase-3 and its physiological substrate PARP. Similar results were obtained in NB-39-nu cells. Our previous observation also demonstrated that activation and nuclear translocation of caspases were associated with prognosis of primary neuroblastomas (Nakagawara *et al.*, 1997). Therefore, the molecular mechanism(s) of RA-induced activation of caspases in neuroblastoma cells needs to be clarified.

In response to a variety of apoptotic stimuli, p53 is induced to be stabilized and subsequently transactivates a number of proapoptotic genes that encode Bcl-2

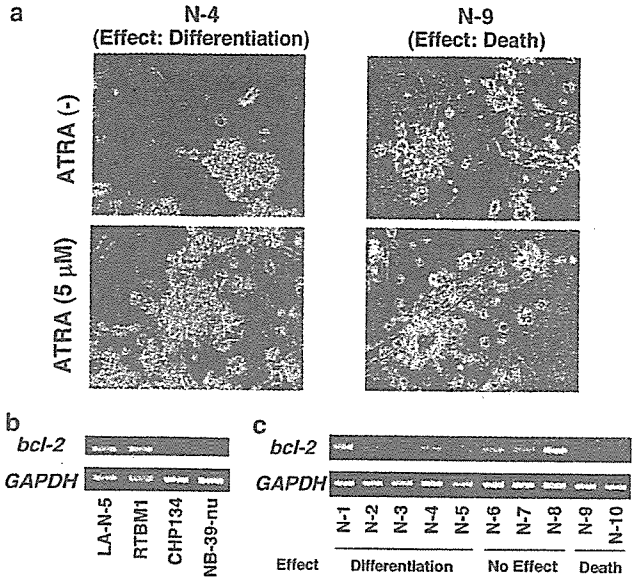

Figure 5 Primary culture and *bcl-2* expression of sporadic neuroblastomas. (a) Primary tumor cells prepared from 10 sporadically found neuroblastoma tissues were cultured with or without 5 μM of ATRA. After 4 days, cells were examined by phase-contrast microscope, and morphological changes of two representative cases are shown. (b and c) RT–PCR analysis. Total RNA was purified from the indicated neuroblastoma cell lines (b) and fresh-frozen tissues of primary neuroblastomas (c), and subjected to RT–PCR using specific primers for *bcl-2*. N-1 to N-10 indicates the case numbers, and the effects of ATRA on primary cultures are described at the bottom of this panel. Glyceraldehyde-3-phosphate dehydrogenase (*GAPDH*) expression is shown as an internal control.

family proteins including Bax (Culmsee and Mattson, 2005). It has been well documented that Bax acts on the mitochondria to induce mitochondrial permeability transition, and thereby regulating the cytoplasmic release of cytochrome *c* (Antonsson, 2001). Neuroblastoma cell lines that we examined in this study carry wild-type p53. Under our experimental conditions, however, we could not detect the ATRA-mediated upregulation of the endogenous p53 as well as Bax. Similarly, the p53-responsible $p21^{WAF1}$ and proapoptotic Puma were not accumulated in response to ATRA. As described (Nikolaev *et al.*, 2003), p53 might not be functional in neuroblastoma cells due to its abnormal cytoplasmic retention. Consistent with this notion, p53 was predominantly expressed in the cytoplasm of neuroblastoma cells examined in this study (data not shown). We have previously shown that cytoplasmic p53 is translocated into the nucleus of CHP134 cells in response to ATRA (Takada *et al.*, 2001); however, our present results suggest that translocated p53 was not functional. Indeed, it is reported that p53 in neuroblastoma cells is not functional even after its enforced translocation into the nucleus (Ostermeyer *et al.*, 1996). Thus, it is likely that the ATRA-mediated apoptotic cell death in neuroblastoma cells is regulated in a p53-independent manner.

Among other regulators of mitochondrial pathway of apoptosis, Bcl-2 family proteins are critical determinants of mitochondrial membrane potential, which controls the cytoplasmic release of cytochrome *c* from mitochondria and thereby regulating apoptotic cell death (Cory *et al.*, 2003). They are divided into two subfamilies based on their biological roles. Antiapoptotic subfamily includes Bcl-2 and Bcl-x_L and proapoptotic subfamily includes Bax, Bim and Bmf. The balance between these two groups determines the fate of cells. Antiapoptotic Bcl-2 is one of the most important members that inhibits the mitochondria-dependent apoptotic pathway triggered by diverse cytotoxic agents through blocking mitochondrial permeability transition. Indeed, the upregulation of Bcl-2 was associated with the drug-resistant phenotype of certain human tumors (Dole *et al.*, 1994; Lombet *et al.*, 2001). Most intriguingly, our expression studies revealed that antiapoptotic Bcl-2 was constitutively overexpressed in LA-N-5 and RTBM1 cells, whereas its expression levels were extremely low in CHP134 and NB-39-nu cells. In response to ATRA, Bcl-2 was slightly induced to be accumulated in NB-39-nu cells; however, it was maintained at extremely low levels in CHP134 cells. Furthermore, two primary neuroblastomas on which ATRA had toxic effect in primary culture did not express *bcl-2*, similar to CHP134 and NB-39-nu cells. Interestingly, ATRA induced differentiation in five cases and had undetectable effects on three cases, but cell death was induced in two cases. Considering that RA treatment contributed to survival of 17% of patients with aggressive neuroblastomas (Matthay *et al.*, 1999), our present results using primary neuroblastomas seem to be reliable. Taken together, it is likely that ATRA potentially have toxic effect on certain neuroblastoma cells (both primary cells and cell lines) that express little Bcl-2. Our current results also revealed that enforced expression of Bcl-2 in CHP134 cells inhibited the ATRA-mediated apoptosis in association with the activation of caspase-3. Furthermore, ATRA treatment of RTBM1 cells followed by HA14-1 exposure underwent apoptotic cell death through mitochondrial pathway. These observations also support the importance of Bcl-2 in the regulation of apoptotic response of neuroblastoma cells to RA.

Although it is still unclear whether the expression levels of Bcl-2 could be correlated with the prognosis of neuroblastoma patients (Romani and Lu, 1994; Gallo *et al.*, 2003; Abel *et al.*, 2005), it is possible that Bcl-2 plays a key role at least in part in the regulation of ATRA-mediated apoptotic cell death in neuroblastoma cells. In this connection, the antisense RNA-mediated knockdown of the endogeneous Bcl-2 has been employed to treat certain tumors (Kim *et al.*, 2004). Recently, a novel Bcl-2 inhibitor that has an antitumor effect on solid tumors has been developed (Oltersdorf *et al.*, 2005). Based on our present findings, the combination of RA with Bcl-2-specific inhibitor might provide a novel therapeutic strategy for the treatment of neuroblastomas, instead of the classical chemotherapy that frequently has multi-organ side effects.

Materials and methods

Cell lines and transfection

Human neuroblastoma-derived cell lines, including LA-N-5, RTBM1, CHP134 and NB-39-nu, were maintained in RPMI 1640 medium supplemented with 10% heat-inactivated fetal bovine serum, penicillin (50 U/ml) and streptomycin (50 μg/ml) at 37°C in a humidified atmosphere of 5% CO_2 in the air. For transfection, CHP134 cells were transfected with the expression plasmid encoding human Bcl-2 or with the empty plasmid by electroporation using a Nucleofector (Amaxa Biosystems, Koeln, Germany) according to the manufacturer's protocol.

Reagents

All-*trans* retinoic acid was purchased from Sigma (St Louis, MO, USA) dissolved in dimethylsulfoxisde (DMSO) at a final concentration of 5 mM, and kept at −80°C. Bcl-2 inhibitor HA14-1 was purchased from Sigma, dissolved in DMSO as a 10 mM stock solution and stored at −20°C. All reagents were of the highest quality available.

Proliferation assay

LA-N-5 and RTBM1 cells were plated in triplicate at a density of 1×10^5 per well in 12-well culture plates. CHP134 and NB-39-nu cells were seeded in triplicate at a density of 1×10^4 in 12-well plates. Twelve hours after seeding the cells, cells were treated with ATRA at a final concentration of 5 μM or left untreated, and medium was replaced every 2 days. At the indicated time points after the treatment with ATRA, cells were trypsinized and number of viable cells was directly scored by using the hemocytometer.

Flow cytometric analysis

Cells were exposed to the indicated concentration of ATRA. At the indicated time points after the treatment with ATRA, cells were collected by brief centrifugation, and fixed with 70% ethanol at −20°C. The cells were washed with phosphate-buffered saline (PBS), resuspended in phosphate-citrate buffer (4 mM citric acid, 200 mM Na_2HPO_4) and kept at room temperature for 15 min. The cells were then centrifuged and resuspended in a solution containing 40 μg/ml of propidium iodide and 0.05% RNase A, and incubated in the dark for 30 min. Before performing flow cytometric analysis, cells were filtered through a 40-μm nylon mesh. DNA content was analysed by FACScan flow cytometer (Becton Dickinson, Oxford, UK).

Immunoblot analysis

Cells were washed twice with ice-cold PBS, lysed in a sodium dodecyl sulfate (SDS)-sample buffer containing 10% glycerol, 5% β-mercaptoethanol, 2.3% SDS and 62.5 mM Tris-HCl, pH 6.8, and then boiled for 3 min. The protein concentrations were determined using Bio-Rad protein assay dye reagent (Bio-Rad Laboratories, Hercules, CA, USA). Bovine serum albumin (BSA) was used as a standard. Aliquots (20 μg) of whole-cell lysates were separated by SDS–polyacrylamide gel electrophoresis and electrophoretically transferred onto polyvinylidene difluoride membranes (Immobilon-P, Millipore, Bedford, MA, USA). The membranes were blocked with 0.3% non-fat milk in Tris-buffered saline containing 0.1% Tween-20 and incubated with appropriate primary antibodies at room temperature for 1 h followed by incubation with the horseradish peroxidase-conjugated secondary antibodies (Cell Signaling Technology Inc., Beverly, MA, USA). Immunoreactive bands were visualized by using ECL system (Amersham Biosciences, Uppsala, Sweden). The primary antibodies used in this study were as follows: polyclonal anti-caspase-12 (Cell Signalling Technology Inc.), polyclonal anti-caspase-3 (Calbiochem, San Diego, CA, USA), polyclonal anti-PARP (Cell Signaling Technology Inc.), polyclonal anti-PUMA (ab9643; Abcam, Cambridge, UK), polyclonal anti-$p21^{WAF1}$ (H-164; Santa Cruz Biotechnology), polyclonal anti-Bim (Cell Signaling Technology Inc.), polyclonal anti-Bmf (Cell Signaling Technology Inc.), polyclonal anti-actin (20-33; Sigma), monoclonal anti-caspase-8 (5F7; Medical & Biological Laboratories, Nagoya, Japan), monoclonal anti-caspase-9 (5B4; Medical & Biological Laboratories), monoclonal anti-p53 (DO-1; Oncogene Research Products, Cambridge, MA, USA), monoclonal anti-Bax (6A7; eBioscience, San Diego, CA, USA), monoclonal anti-Bcl-2 (100; Santa Cruz Biotechnology); and monoclonal anti-Bcl-x_L (H-5; Santa Cruz Biotechnology) antibodies.

Immunofluorescent staining

CHP134 cells were grown on coverslips in standard culture medium in the presence or absence of 5 μM of ATRA for 4 days. Cells were washed with ice-cold PBS, fixed with 3.7% formaldehyde in PBS for 30 min, permeabilized with 0.2% Triton X-100 in PBS for 5 min and then blocked with 3% BSA in PBS for 1 h at room temperature. After blocking, cells were incubated with a monoclonal antibody against cytochrome *c* (6H2.B4; BD PharMingen, San Jose, CA, USA) or with a normal mouse IgG for 1 h at room temperature, followed by the incubation with fluorescein isothiocyanate-conjugated secondary antibody against mouse IgG (Santa Cruz Biotechnology). The cell nuclei were stained with DAPI. The coverslips were mounted onto glass slides, and the stained cells were examined by using a confocal laser scanning microscope (Olympus).

Primary culture

RPMI 1640 medium supplemented with 10% heat-inactivated fetal bovine serum, penicillin (50 U/ml), streptomycin (50 μg/ml) and 100 μg/ml of OPI (Sigma) was used as a standard medium for primary culture. Primary tumor cells were prepared from fresh human neuroblastoma tissues by a standard method. A total of 5×10^5 cells of each sample were resuspended in 1 ml of the standard medium, and seeded on 24-well tissue culture plates precoated with collagen. The cells were treated with or without ATRA at a final concentration of 5 μM for at least 2 weeks. The effects of ATRA on the growth and neurite extension of primary neuroblastoma cells were examined by phase-contrast microscope.

RNA extraction and RT–PCR

Total RNA was prepared from fresh-frozen tissues of primary neuroblastomas or cultured cells by using RNeasy Mini Kit (Qiagen, Valencia, CA, USA). Total RNA (2 μg) was reverse transcribed by using random primers and SuperScript II reverse transcriptase (Invitrogen, Carlsbad, CA, USA). The resultant cDNA was subjected to PCR-based amplification. The oligonucleotide primers used in this study were as follows: *bcl-2*, 5′-GAGGATTGTGGCCTTCTTTG-3′ (forward) and 5′-ACAGTTCCACAAAGGCATCC-3′ (reverse), and glyceraldehyde-3-phosphate dehydrogenase (*GAPDH*), 5′-ACCTGA CCTGCCGTCTAGAA-3′ (forward) and 5′-TCCACCACCC TGTTGCTGTA-3′ (reverse). PCR products were electrophoretically separated on 1% neutral agarose gels and visualized by ethidium bromide staining.

Acknowledgements

We are grateful to the hospitals and institutions that provided us with surgical specimens. We thank Hideki Yamamoto and Atsushi Kawasaki for valuable discussions, and Yuki Nakamura for excellent technical assistance. This work was supported in part by a Grant-in-Aid from the Ministry of Health, Labour and Welfare for Third Term Comprehensive Control Research for Cancer, and a Grant-in-Aid for Scientific Research on Priority Areas and a Grant-in-Aid for Scientific Research (C) from the Ministry of Education, Culture, Sports, Science and Technology, Japan.

References

Abel F, Sjoberg RM, Nilsson S, Kogner P, Martinsson T. (2005). *Eur J Cancer* **41**: 635–646.
Antonsson B. (2001). *Cell Tissue Res* **306**: 347–361.
Balmer JE, Blomhoff R. (2002). *J Lipid Res* **43**: 1773–1808.
Brodeur GM. (2003). *Nat Rev Cancer* **3**: 203–216.
Brodeur GM, Nakagawara A. (1992). *Am J Pediatr Hematol Oncol* **14**: 111–116.
Cory S, Huang DC, Adams JM. (2003). *Oncogene* **22**: 8590–8607.
Culmsee C, Mattson MP. (2005). *Biochem Biophys Res Commun* **331**: 761–777.
Degterev A, Boyce M, Yuan J. (2003). *Oncogene* **22**: 8543–8567.
Dole M, Nunez G, Merchant AK, Maybaum J, Rode CK, Bloch CA *et al.* (1994). *Cancer Res* **54**: 3253–3259.
Encinas M, Iglesias M, Llecha N, Comella JX. (1999). *J Neurochem* **73**: 1409–1421.
Freemantle SJ, Spinella MJ, Dmitrovsky E. (2003). *Oncogene* **22**: 7305–7315.
Gallo G, Giarnieri E, Bosco S, Cappelli C, Alderisio M, Giovagnoli MR *et al.* (2003). *Anticancer Res* **23**: 777–784.
Kim R, Emi M, Tanabe K, Toge T. (2004). *Cancer* **101**: 2491–2502.
Lee MH, Nikolic M, Baptista CA, Lai E, Tsai LH, Massague J. (1996). *Proc Natl Acad Sci USA* **93**: 3259–3263.
Lippman SM, Lotan R. (2000). *J Nutr* **130**: 479S–482S.
Lombet A, Zujovic V, Kandouz M, Billardon C, Carvajal-Gonzalez S, Gompel A *et al.* (2001). *Eur J Biochem* **268**: 1352–1362.
Lopez-Carballo G, Moreno L, Masia S, Perez P, Barettino D. (2002). *J Biol Chem* **277**: 25297–25304.
Maden M. (2001). *Int Rev Cytol* **209**: 1–77.
Matthay KK, Villablanca JG, Seeger RC, Stram DO, Harris RE, Ramsay NK *et al.* (1999). *N Engl J Med* **341**: 1165–1173.
McCaffery PJ, Adams J, Maden M, Rosa-Molinar E. (2003). *Eur J Neurosci* **18**: 457–472.
Melino G, Thiele CJ, Knight RA, Piacentini M. (1997). *J Neurooncol* **31**: 65–83.
Morishima N, Nakanishi K, Takenouchi H, Shibata T, Yasuhiko Y. (2002). *J Biol Chem* **277**: 34287–34294.
Nagai J, Yazawa T, Okudela K, Kigasawa H, Kitamura H, Osaka H. (2004). *Cancer Res* **64**: 7910–7917.
Nakagawa T, Zhu H, Morishima N, Li E, Xu J, Yankner BA *et al.* (2000). *Nature* **403**: 98–103.
Nakagawara A. (1998). *Hum Cell* **11**: 115–124.
Nakagawara A, Arima-Nakagawara M, Scavarda NJ, Azar CG, Cantor AB, Brodeur GM. (1993). *N Engl J Med* **328**: 847–854.
Nakagawara A, Azar CG, Scavarda NJ, Brodeur GM. (1994). *Mol Cell Biol* **14**: 759–767.
Nakagawara A, Nakamura Y, Ikeda H, Hiwasa T, Kuida K, Su MS *et al.* (1997). *Cancer Res* **57**: 4578–4584.
Nakamura Y, Ozaki T, Koseki H, Nakagawara A, Sakiyama S. (2003). *Biochem Biophys Res Commun* **307**: 206–213.
Nikolaev AY, Li M, Puskas N, Qin J, Gu W. (2003). *Cell* **112**: 29–40.
Okuno S, Saito A, Hayashi T, Chan PH. (2004). *J Neurosci* **24**: 7879–7887.
Oltersdorf T, Elmore SW, Shoemaker AR, Armstrong RC, Augeri DJ, Belli BA *et al.* (2005). *Nature* **435**: 677–681.
Ostermeyer AG, Runko E, Winkfield B, Ahn B, Moll UM. (1996). *Proc Natl Acad Sci USA* **93**: 15190–15194.
Piacentini M, Annicchiarico-Petruzzelli M, Oliverio S, Piredda L, Biedler JL, Melino G. (1992). *Int J Cancer* **52**: 271–278.
Puthalakath H, Villunger A, O'Reilly LA, Beaumont JG, Coultas L, Cheney RE *et al.* (2001). *Science* **293**: 1829–1832.
Reynolds CP, Lemons RS. (2001). *Hematol Oncol Clin N Am* **15**: 867–910.
Romani P, Lu QL. (1994). *J Pathol* **172**: 273–278.
Schor NF. (1999). *J Neurooncol* **41**: 159–166.
Shi L, Gong S, Yuan Z, Ma C, Liu Y, Wang C *et al.* (2004). *Neurosci Lett* **375**: 7–12.
Takada N, Isogai E, Kawamoto T, Nakanishi H, Todo S, Nakagawara A. (2001). *Med Pediatr Oncol* **36**: 122–126.
Teitz T, Wei T, Valentine MB, Vanin EF, Grenet J, Valentine VA *et al.* (2000). *Nat Med* **6**: 529–535.
Thiele CJ, Reynolds CP, Israel MA. (1985). *Nature* **313**: 404–406.
Van Noesel MM, Van Bezouw S, Voute PA, Herman JG, Pieters R, Versteeg R. (2003). *Genes Chromosomes Cancer* **38**: 226–233.
Van Noesel MM, Versteeg R. (2004). *Gene* **325**: 1–15.
Villablanca JG, Khan AA, Avramis VI, Seeger RC, Matthay KK, Ramsay NK *et al.* (1995). *J Clin Oncol* **13**: 894–901.
Wang JL, Liu D, Zhang ZJ, Shan S, Han X, Srinivasula SM *et al.* (2000). *Proc Natl Acad Sci USA* **97**: 7124–7129.